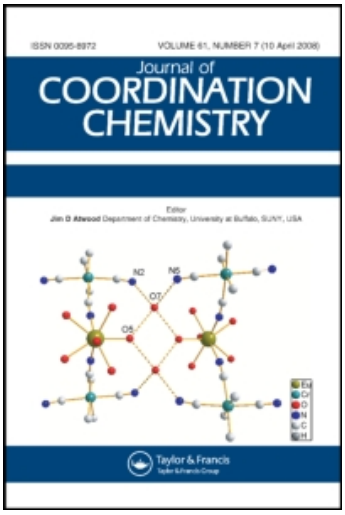

Journal of Coordination Chemistry
Publication details, including instructions for authors and subscription information:
http://www.informaworld.com/smpp/title~content=t713455674

Syntheses, crystal structures, fluorescent, and thermal properties of nickel(II) 5,5-diethylbarbiturate complexes with (2-aminomethyl), (2-aminoethyl), and (2-hydroxyethyl)pyridines

Veysel T. Yilmaz[a]; Fatih Yilmaz[b]; Emel Guney[a]; Orhan Buyukgungor[c]
[a] Department of Chemistry, Faculty of Arts and Sciences, Uludag University, 16059 Bursa, Turkey [b] Department of Chemistry, Faculty of Arts and Sciences, Rize University, 53100 Rize, Turkey [c] Department of Physics, Faculty of Arts and Sciences, Ondokuz Mayis University, 55139 Samsun, Turkey

First published on: 30 November 2010

To cite this Article Yilmaz, Veysel T. , Yilmaz, Fatih , Guney, Emel and Buyukgungor, Orhan(2011) 'Syntheses, crystal structures, fluorescent, and thermal properties of nickel(II) 5,5-diethylbarbiturate complexes with (2-aminomethyl), (2-aminoethyl), and (2-hydroxyethyl)pyridines', Journal of Coordination Chemistry, 64: 1, 159 — 169, First published on: 30 November 2010 (iFirst)
To link to this Article: DOI: 10.1080/00958972.2010.537333
URL: http://dx.doi.org/10.1080/00958972.2010.537333

Journal of Coordination Chemistry
Vol. 64, No. 1, 10 January 2011, 159–169

Syntheses, crystal structures, fluorescent, and thermal properties of nickel(II) 5,5-diethylbarbiturate complexes with (2-aminomethyl), (2-aminoethyl), and (2-hydroxyethyl)pyridines

VEYSEL T. YILMAZ*†, FATIH YILMAZ‡,
EMEL GUNEY† and ORHAN BUYUKGUNGOR§

†Department of Chemistry, Faculty of Arts and Sciences,
Uludag University, 16059 Bursa, Turkey
‡Department of Chemistry, Faculty of Arts and Sciences,
Rize University, 53100 Rize, Turkey
§Department of Physics, Faculty of Arts and Sciences,
Ondokuz Mayis University, 55139 Samsun, Turkey

(*Received 24 August 2010; in final form 22 September 2010*)

Three nickel(II) complexes of 5,5-diethlybarbiturate (barb) with (2-aminomethyl)pyridine (ampy), (2-aminoethyl)pyridine (aepy), and (2-hydroxyethyl)pyridine (hepy), [Ni(barb-*N*)$_2$(ampy)$_2$] (**1**), [Ni(barb-*N*,*O*)(aepy)$_2$](barb)·H$_2$O (**2**), and [Ni(barb-*O*)$_2$(hepy)]·2H$_2$O (**3**), have been synthesized and characterized by elemental analysis, IR, thermal analysis, and single crystal X-ray diffraction. All complexes are mononuclear with nickel(II) exhibiting an octahedral coordination. Ampy, aepy, and hepy are bidentate chelating ligands, while barb shows different coordination modes. In **1**, two barb ligands are *N*-bonded, whereas in **3** they are *O*-coordinated through one carbonyl oxygen. In **2**, one barb is bidentate chelating, while the second barb remains outside the coordination sphere as a counterion. The molecules of **1**–**3** are bridged by multiple hydrogen bonds to generate 1-D or 2-D supramolecular networks. All complexes are fluorescent due to π–π^* transitions.

Keywords: 5,5-Diethylbarbiturate; (2-Aminomethyl)pyridine; (2-Aminoethyl)pyridine; (2-Hydroxyethyl)pyridine; Nickel(II)

1. Introduction

Barbital (barb), known as 5,5-diethylbarbiturate or 5,5-diethyl-2,4,6(1H,3H,5H)-pyrimidine-trione, has been used widely as a sedative and hypnotics agent [1–4]. Barbital has strong inhibiting effect on the central nervous system [5]. Because of the wide range of medicinal applications of barb and its ability to coordinate to transition metals, synthesis of its metal complexes has attracted considerable attention and several metal complexes of barb have been appeared in the literature [6–10]. The barb monoanion in these complexes is monodentate through the deprotonated nitrogen.

*Corresponding author. Email: vtyilmaz@uludag.edu.tr

Journal of Coordination Chemistry
ISSN 0095-8972 print/ISSN 1029-0389 online © 2011 Taylor & Francis
DOI: 10.1080/00958972.2010.537333

Recently, a dinuclear complex [{$Re(CO)_5$}$_2$(barb)] containing a bridging barb dianion has been reported [11].

As part of our interest on the metal complexes of 5,5-diethylbarbituratic acid (barbH), in addition to the usual N-coordination of barb, we observed that this ligand shows various coordination modes, such as bidentate chelating ligand *via* the negatively charged nitrogen and one carbonyl oxygen [12, 13] and bidentate or tridentate bridging [14–16]. Unequal coordination of the barb ligands (one monodentate (N) and one bidentate (N, O)) around the same coordination sphere was also observed [13, 17]. Among the metal complexes of barb, nickel(II) complexes have received less attention and only a nickel(II) complex of 5-ethyl-5-isoamylbarbiturate with imidazole was reported [18]. In this article, we report the synthesis and characterization of three new barb complexes of nickel(II) with (2-aminomethyl)pyridine (ampy), (2-aminoethyl)pyridine (aepy), and (2-hydroxyethyl)pyridine (hepy), [Ni(barb-*N*)$_2$(ampy)$_2$] (**1**), [Ni(barb-*N*,*O*)(aepy)$_2$](barb)·H_2O (**2**), and [Ni(barb-*O*)$_2$(hepy)]·$2H_2O$ (**3**). Spectroscopic properties, fluorescence, and thermal behaviors of these complexes are discussed. In addition, new coordination modes of barb were established by single-crystal X-ray diffraction studies.

2. Experimental

2.1. *Materials and measurements*

Elemental analyses were determined on a Costech elemental analyser. IR spectra were recorded with a Thermo Nicolet 6700 FT-IR spectrophotometer with samples as KBr pellets from 4000 to 400 cm^{-1}. Electronic spectra were measured on a Shimadzu UV-2100 from 200 to 900 nm. Luminescence spectra of 1×10^{-3} mol L^{-1} DMF solutions were recorded at room temperature with a Varian Cary Eclipse spectrophotometer equipped with a Xe pulse lamp of 75 kW. Thermal analysis curves (TGA and DTA) were obtained using a Seiko Exstar 6200 thermal analyzer in a dynamic air atmosphere with a heating rate of 10°C min^{-1} and a sample size of *ca* 10 mg.

2.2. *Synthesis of the nickel(II) complexes*

Complexes **1**–**3** were prepared using the same synthesis procedure. A solution of Na(barb) (5,5-diethylbarbituric acid sodium salt) (4 mmol, 0.82 g) in distilled water (10 mL) was mixed with a 10 mL aqueous solution of $NiSO_4 \cdot 6H_2O$ (2 mmol, 0.53 g) with stirring; a green precipitate was formed. Ampy (4 mmol) was added dropwise to the suspension and subsequently 10 mL 2-propanol was added. This resulted in a clear solution. A similar procedure was repeated for aepy and hepy. The reaction mixtures were stirred for 30 min at room temperature. The final solutions were allowed to stand at room temperature and X-ray quality crystals of **1**–**3** were formed after 2 days.

[Ni(barb-*N*)$_2$(ampy)$_2$] (**1**): Yield 82%; m.p. 212°C (decomposition). Anal. Calcd for $C_{28}H_{38}N_8O_6Ni$ (%): C, 52.4; H, 6.0; N, 17.5. Found (%): C, 52.7; H, 5.8; N, 17.5. (Solid KBr pellet): ν (cm^{-1}) 3342m, 3255sh, 3157sb, 3103vw, 3054w, 2976m, 2931m, 2875vw, 2829vw, 1703vs, 1651vs, 1587vs, 1563vs, 1439s, 1409vs, 1355vs, 1316vs, 1296vs, 1247vs,

1170w, 1152w, 1050m, 1020w, 987s, 918m, 860s, 784m, 746vs, 724m, 689m, 612w, 467m, 436w.

[Ni(barb-*N*,*O*)(aepy)$_2$](barb)·H_2O (**2**): Yield 66%; m.p. 167°C (decomposition). Anal. Calcd for $C_{30}H_{44}N_8O_7Ni$ (%): C, 52.4; H, 6.5; N, 16.3. Found (%): C, 52.6; H, 6.4; N, 16.5. IR (Solid KBr pellet): ν (cm^{-1}) 3454m, 3356w, 3295m, 3225w, 3167sb, 3061w, 2968m, 2931m, 2874w, 2813w, 1686s, 1673vs, 1560vs, 1547vs, 1443m, 1421m, 1408m, 1333s, 1305vs, 1264vs, 1165m, 1146m, 1064w, 946m, 831w, 781m, 756s, 679w, 501m, 463w.

[Ni(barb-*O*)$_2$(hepy)]·$2H_2O$ (**3**): Yield 57%; m.p. 143°C (decomposition). Anal. Calcd for $C_{30}H_{44}N_6O_{10}Ni$ (%): C, 50.9; H, 6.3; N, 11.9. Found (%): C, 51.1; H, 6.2; N, 12.0. (Solid KBr pellet): ν (cm^{-1}) 3445m, 3154wb, 3040m, 2967m, 2904w, 2870w, 2840w, 1665vs, 1658vs, 1606m, 1571m, 1534vs, 1421vs, 1386vs, 1335vs, 1309vs, 1270vs, 1185w, 1106w, 1115w, 1082w, 1065m, 1025s, 988s, 965s, 906w, 887m, 855w, 787m, 775s, 755m, 692w, 636m, 514m, 449w.

2.3. *X-ray crystallography*

Intensity data of **1**–**3** were collected using a STOE IPDS 2 diffractometer with graphite-monochromated Mo-Kα radiation ($\lambda = 0.71073$) at 295 K. The structures were solved by direct methods and refined on F^2 with the SHELXL-97 program [19]. All non-hydrogen atoms were found from the difference Fourier map and refined anisotropically. The OH hydrogens were refined freely, while other hydrogens were included using a riding model. The details of data collection, refinement, and crystallographic data are summarized in table 1.

3. Results and discussion

3.1. *Synthesis and IR characterization*

The reaction of Na(barb) with $NiSO_4 \cdot 6H_2O$ in the presence of ampy, aepy, and hepy yielded **1**–**3** in moderate yields (over 55%). The analytical data (C, H, and N) are consistent with the proposed empirical formulation, which is also confirmed by single crystal X-ray analysis. All three complexes are soluble in DMSO, DMF, warm water, and EtOH.

Selected IR spectral data are summarized in table 2. Bands centered at 3450 cm^{-1} are attributed to OH vibrations in **2** and **3**. Two absorption bands between 3225 and 3342 cm^{-1} are due to symmetric and asymmetric stretches of NH_2 of the amine ligands in **1** and **2**, while bands ranging from 3154 to 3167 cm^{-1} are assigned to NH groups of barb. Two sharp absorptions between 1651 and 1703 cm^{-1} are characteristic for carbonyl groups of barb, in agreement with the presence of different carbonyl groups involved in coordination or strong hydrogen bonding. Strong bands in the range of 1247–1270 cm^{-1} are assigned to ν(C–N).

3.2. *Crystal structures*

The molecular structures of **1**–**3** are shown in figures 1–3. Selected bond lengths and angles together with hydrogen bonding geometry are listed in tables 3–5. All three

Table 1. Crystallographic data and structure refinement for **1**–**3**.

	1	**2**	**3**
Empirical formula	$C_{28}H_{38}N_8O_6Ni$	$C_{30}H_{44}N_8O_7Ni$	$C_{30}H_{44}N_6O_{10}Ni$
Formula mass	641.37	687.44	707.42
Crystal system	Triclinic	Monoclinic	Triclinic
Space group	$P\bar{1}$	$P21/c$	$P\bar{1}$
Unit cell dimensions (Å, °)			
a	7.4653(11)	10.2355(4)	8.0994(4)
b	9.7332(13)	16.8668(8)	9.8681(5)
c	11.3466(16)	20.0490(9)	10.9494(6)
α	78.960(12)	90	82.203(4)
β	74.252(11)	94.773(3)	85.919(5)
γ	70.825(11)	90	77.455(4)
Volume (Å^3), Z	744.72(18), 1	3449.3(3), 4	845.56(8), 1
Calculated density (g cm^{-3})	1.430	1.324	1.389
Absorption coefficient (mm^{-1})	0.707	0.618	0.637
$F(000)$	338	1456	374
Crystal size (mm^3)	$0.57 \times 0.36 \times 0.13$	$0.25 \times 0.19 \times 0.15$	$0.42 \times 0.29 \times 0.13$
θ range for data collection (°)	2.75–26.50	1.58–26.70	2.58–26.50
Index range (h, k, l)	−8/9, −12/12, −14/14	−12/12, −21/21, −25/25	−10/10, −12/12, −13/13
Reflections collected	6879	52094	12918
Independent reflection	3070 ($R_{int} = 0.0431$)	7261 ($R_{int} = 0.0968$)	3508 ($R_{int} = 0.0339$)
Absorption correction	Numerical	Numerical	Numerical
Data/parameters	3070/196	7261/423	3508/224
Goodness-of-fit on F^2	1.139	0.0828	1.051
Final R indices [$I > 2\sigma(I)$]	0.0369	0.0350	0.0258
$\Delta\rho_{max/min}$ (e Å^{-3})	0.611/−0.433	0.237/−0.316	0.289/−0.268

Table 2. Selected IR spectral data for **1**–**3**.[a]

Assignments	**1**	**2**	**3**
ν(OH)	–	3454m, 3356w	3445m
ν(NH)amine	3342m, 3250sb	3295m, 3225w	–
ν(NH)barb	3157sb	3167sb	3154sb
ν(CH)	3103–2829w	3061–2813w	3073–2879w
ν(CO)	1703vs, 1651vs	1686s, 1673vs	1665vs, 1658vs
ν(CN)	1587vs, 1247vs	1560vs, 1264vs	1606m, 1270vs

[a]Frequencies in cm^{-1}; b = broad; w = weak; vs = very strong; s = strong; sh = shoulder; m = medium.

complexes crystallize as mononuclear species. In **1**, the nickel(II) lies on the center of symmetry and is octahedrally coordinated to two ampy and two barb ligands (figure 1a). The barb ligands are *N*-bonded, while the ampy ligands are bidentate chelating through their nitrogens forming five-membered chelate rings. As shown in figure 2(a), complex **2** consists of a cation $[Ni(barb)(aepy)]^+$, a barb anion, and a lattice water molecule. In the cation, nickel(II) is coordinated by two aepy molecules and a barb anion, forming an octahedral coordination geometry. The aepy ligands are bidentate chelating, creating two six-membered chelate rings. This complex contains two different barb ions; one coordinates copper(II) bidentate *via* the negatively charged N and the carbonyl O, while the second barb remains as a counterion. The simultaneous presence of one coordinated barb and one non-coordinated barb anion in the same compound was observed earlier in $[Cu(barb)(apen)](barb) \cdot 2H_2O$

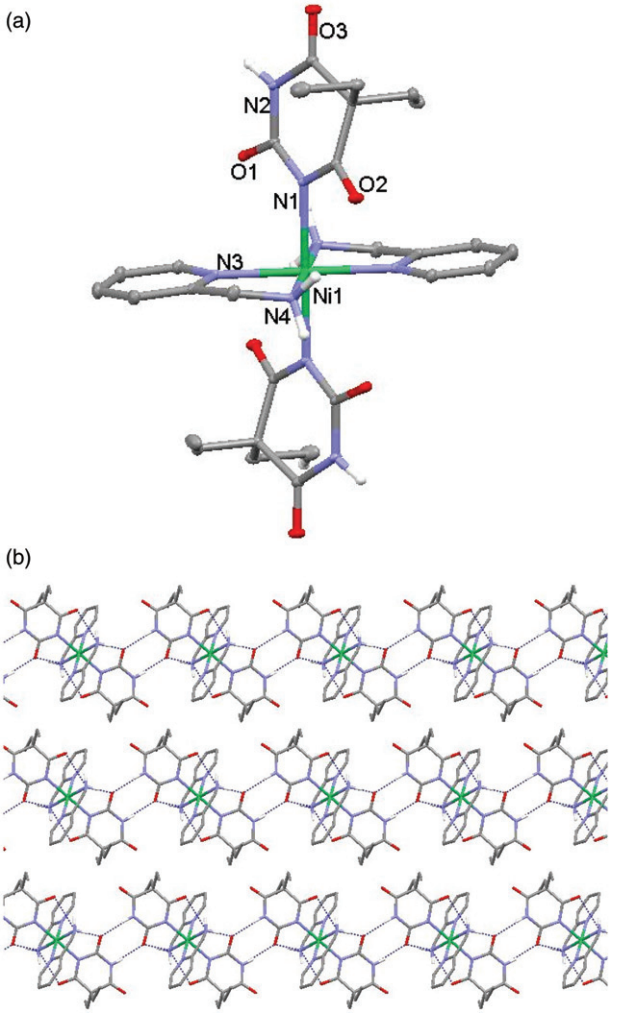

Figure 1. (a) A molecular view of **1** (C–H hydrogens omitted for clarity) and (b) a hydrogen-bonded chain in **1**.

(apen = *N*,*N*′-bis(3-aminopropyl)ethylenediamine) [18], but the barb ligand in the copper(II) complex was monodentate *via* nitrogen. The Ni–N_{barb} bond distances are 2.2252(16) Å in **1** and 2.0933(18) Å in **2**, somewhat longer than those found in the reported nickel(II)–barb complex [2.078(2) Å] [18]. The coordination environment around nickel(II) in **3** is octahedral with a bidentate hepy and two monodentate barb anions (figure 3a). The complex is centrosymmetric as **1**, but the two barb ligands are both *O*-coordinated through carbonyl instead of nitrogen as shown in **1**. To the best of our knowledge, monodentate coordination of barb only *via* the carbonyl oxygen has not been observed until now. The Ni–O_{barb} bond distance in **3** is significantly shorter than in **2**.

Complexes **1**–**3** exhibit multiple intermolecular hydrogen-bonding interactions as listed in tables 3–5. As shown in figure 1(b), the molecules of **1** are doubly bridged by

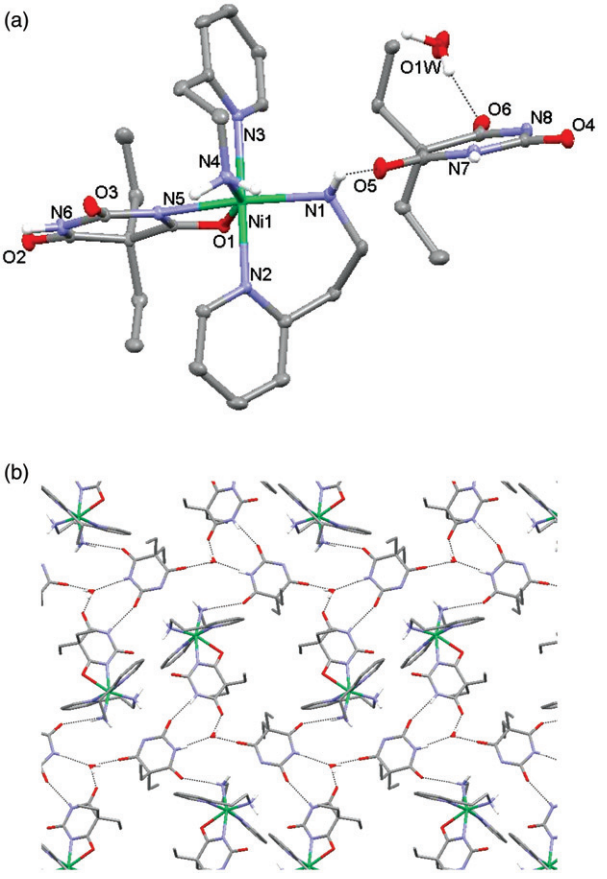

Figure 2. (a) A molecular view of **2** (C–H hydrogens omitted for clarity) and (b) hydrogen-bonded network in **2** viewed down *c*.

N–H···O hydrogen bonds involving the barb moieties into 1-D chains running along the *b*-axis. In **2**, the barb anion and $[Ni(barb)(aepy)]^+$ cation are connected through the **N**–H···O hydrogen bonds into 1-D chains, which are further linked by water bridges into a supramolecular 2-D network, nearly parallel to the *ab* plane (figure 2b). Molecules of **3** are bridged by N–H···OW and OW–H···O hydrogen bonds into a 2-D layer along the *ac* plane (figure 3b).

3.3. *Photoluminescence*

In DMF, all the ligands and their complexes display an absorption band at 268 nm. In addition, aepy shows additional bands at 306 and 344 nm with low intensity. These bands correspond to the absorption of the aromatic moiety and may be assigned to the π–π^* and n–π^* transitions. Excitation of these ligands and metal complexes at the main absorption wavelength (268 nm) does not show any emission band as observed for the corresponding cadmium(II) complexes [20]. However, upon excitation at 315 nm for ampy, 300 nm for aepy, and 360 nm for hepy, these ligands exhibit emission bands at 382, 415, and 440 nm, respectively. As illustrated in figure 4, upon excitation at 315 nm,

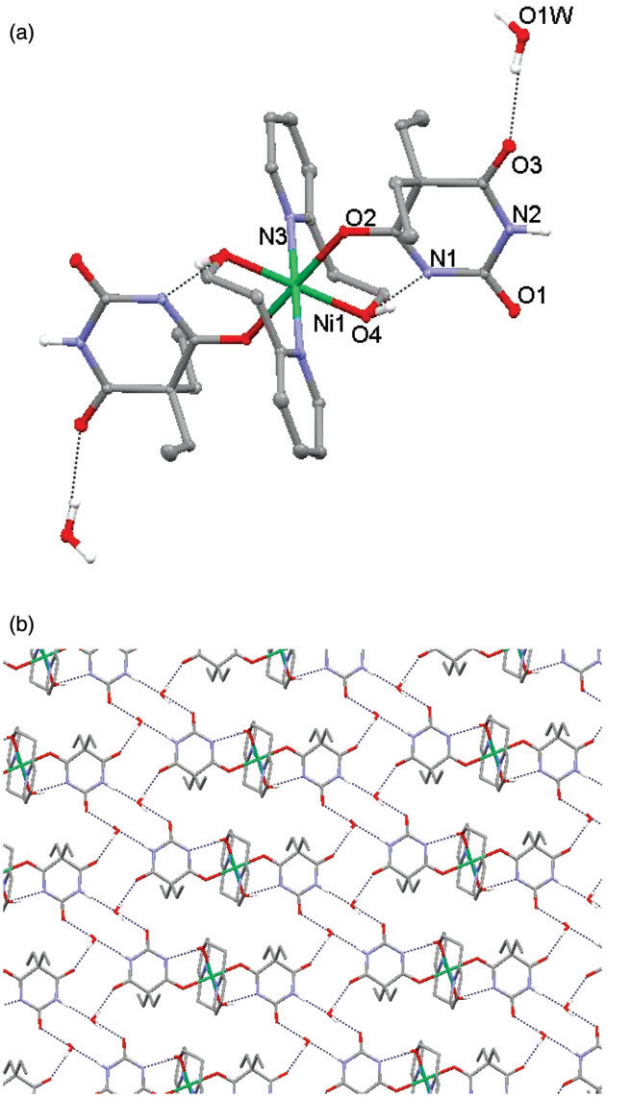

Figure 3. (a) A molecular view of **3** (C–H hydrogens omitted for clarity) and (b) a 2-D layer in **3** viewed down *b*.

1 exhibits two emission maxima at 350 and 370 nm, while **2** is emissive at 375 nm when excited at 310 nm. Complex **3** displays an emission band at 360 nm upon excitation at 305 nm. Compared to the emission spectra free ligands, the metal complexes show a blue shift and the fluorescence of the complexes is due to py-based π–π^* transitions in the excited state [20].

3.4. *Thermal behavior*

The TG and DTA curves of **1**–**3** (figure 5) show a continuous mass loss due to the overlapping of decomposition processes of the co-ligands and barb. However, the

Table 3. Selected bond lengths and angles and hydrogen bonding geometry for **1**.

Bonds lengths (Å) and angles (°)				
Ni1–N1	2.2252(16)	N3–Ni1–N4	79.73(6)	
Ni1–N3	2.1163(16)	N1–Ni1–N3^{i}	90.68(6)	
Ni1–N4	2.0813(16)	N1–Ni1–N4^{i}	88.50(6)	
N1–Ni1–N3	89.32(6)	N3–Ni1–N4^{i}	100.27(6)	
N1–Ni1–N4	91.50(6)			
Hydrogen bonds				
D–H···A	D–H (Å)	H···A (Å)	D···A (Å)	D–H···A (°)
N2–H2···O^{ii}	0.86	1.99	2.850(2)	173
N4–H4A···O2^{i}	0.90	2.09	2.845(2)	141
N4–H4B···O1	0.90	2.18	2.875(2)	134

Symmetry codes: (^{i}) $-x+1, -y+1, -z+1$; (^{ii}) $-x+1, -y, -z+1$.

Table 4. Selected bond lengths and angles and hydrogen bonding geometry for **2**.

Bonds lengths (Å) and angles (°)				
Ni1–N1	2.0757(19)	N2–Ni1–N3	171.52(7)	
Ni1–N2	2.0989(19)	N2–Ni1–N4	94.94(8)	
Ni1–N3	2.1158(19)	N2–Ni1–N5	88.00(7)	
Ni1–N4	2.0475(19)	N2–Ni1–O1	86.62(6)	
Ni1–N5	2.0933(18)	N3–Ni1–N4	93.41(8)	
Ni1–O1	2.2991(15)	N3–Ni1–N5	89.16(7)	
N1–Ni1–N2	90.49(8)	N3–Ni1–O1	85.04(7)	
N1–Ni1–N3	89.78(8)	N4–Ni1–N5	99.73(7)	
N1–Ni1–N4	98.05(8)	N4–Ni1–O1	159.55(7)	
N1–Ni1–N5	162.23(7)	N5–Ni1–O1	59.90(6)	
N1–Ni1–01	102.33(7)			
Hydrogen bonds				
D–H···A	D–H (Å)	H···A (Å)	D···A (Å)	D–H···A (°)
N1–H1B···O6^{i}	0.90	2.47	3.250(3)	145
N1–H1B···N8^{i}	0.90	2.53	3.332(3)	148
N4–H4A···O3^{ii}	0.90	2.44	3.228(3)	147
N4–H4B···O4^{i}	0.90	2.35	3.126(3)	145
N4–H4B···N8^{i}	0.90	2.43	3.221(3)	147
N7–H28···O1W^{i}	0.86	1.89	2.745(3)	172
N6–H6A···O4^{iii}	0.86	2.03	2.863(3)	164
O1W–H1W···O2^{iv}	0.872(18)	1.922(18)	2.784(3)	170(3)
N1–H1A···O5	0.90	2.19	3.013(3)	152
O1W–H2W···O6	0.821(17)	1.870(18)	2.681(3)	169(4)

Symmetry codes: (^{i}) $-x+2, y-1/2, -z+3/2$; (^{ii}) $-x+1, -y, -z+1$; (^{iii}) $x-1, -y+1/2, z-1/2$; (^{iv}) $-x+1, -y+1, -z+1$.

Table 5. Selected bond lengths and angles and hydrogen bonding geometry for **3**.

Bonds lengths (Å) and angles (°)				
Ni1–N3	2.0818(12)	O2–Ni1–O4	92.21(4)	
Ni1–O2	2.0901(9)	N3–Ni1–O2^{i}	94.08(4)	
Ni1–O4	2.0893(9)	N3–Ni1–O4^{i}	89.92(4)	
N3–Ni1–O2	85.92(4)	O2–Ni1–O4^{i}	87.79(4)	
N3–Ni1–O4	90.08(4)			
Hydrogen bonds				
D–H···A	D–H (Å)	H···A (Å)	D···A (Å)	D–H···A (°)
O4–H4···N1	0.83(2)	1.79(2)	2.5921(14)	164(2)
N2–H2···O1W^{ii}	0.86	2.00	2.8479(16)	171
O1W–H5D···O3	0.817(15)	1.971(16)	2.7759(16)	168(3)
O1W–H5C···O1^{iii}	0.864(15)	2.007(17)	2.8526(18)	166(2)

Symmetry codes: (^{i}) $-x+1, -y+1, -z+1$; (^{ii}) $-x, -y+2, -z+2$; (^{iii}) $x-1, y, z$.

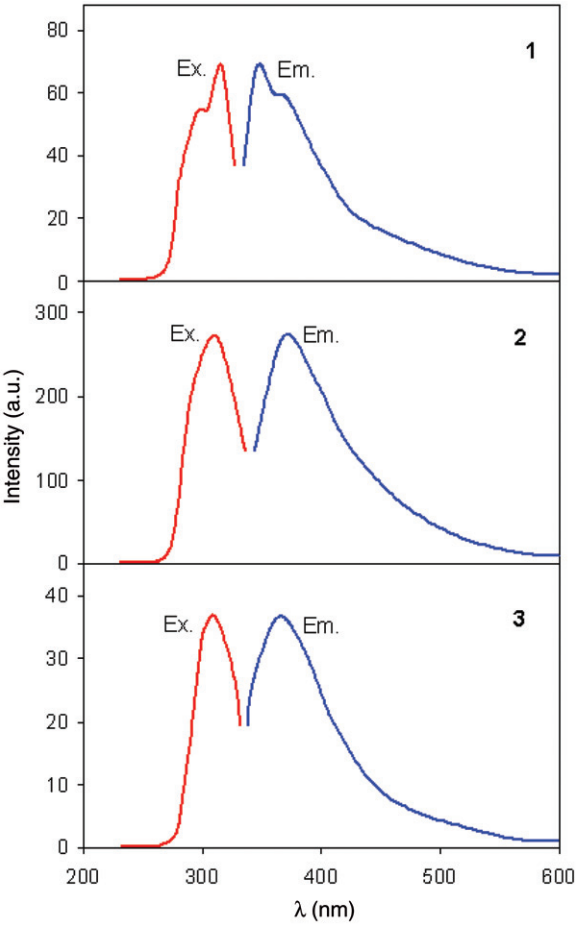

Figure 4. Emission spectra of **1**–**3** in DMF solutions at room temperature.

endo- or exothermic peaks in the DTA indicate the decomposition of the moieties in these complexes.

Complex **1** is stable to 212°C and begins to decompose at higher temperatures. Two endothermic DTA peaks at 264 and 303°C correspond to the elimination of ampy, while a highly exothermic peak centered at 449°C is characteristic for the decomposition of barb. The total mass loss of 88.7% agrees well with the calculated value of 88.3%, corresponding to the end product of NiO at 512°C. Complexes **2** and **3** contain lattice waters. The dehydration of both complexes occurs in the first stage from 99°C to 167°C for **2** and from 83°C to 125°C for **3**. The DTA curve of **2** displays two endothermic peaks at 217 and 323°C for the removal of aepy, while three endothermic peaks between 157 and 248°C are associated with the decomposition of hepy in **3**. The barb ligands decompose exothermically at 451°C for **2** and 468°C for **3** to give NiO as the final decomposition product. Total mass losses of 89.2% for **2** and 89.1% for **3** are consistent with the calculated values of 89.1% and 89.3%, respectively.

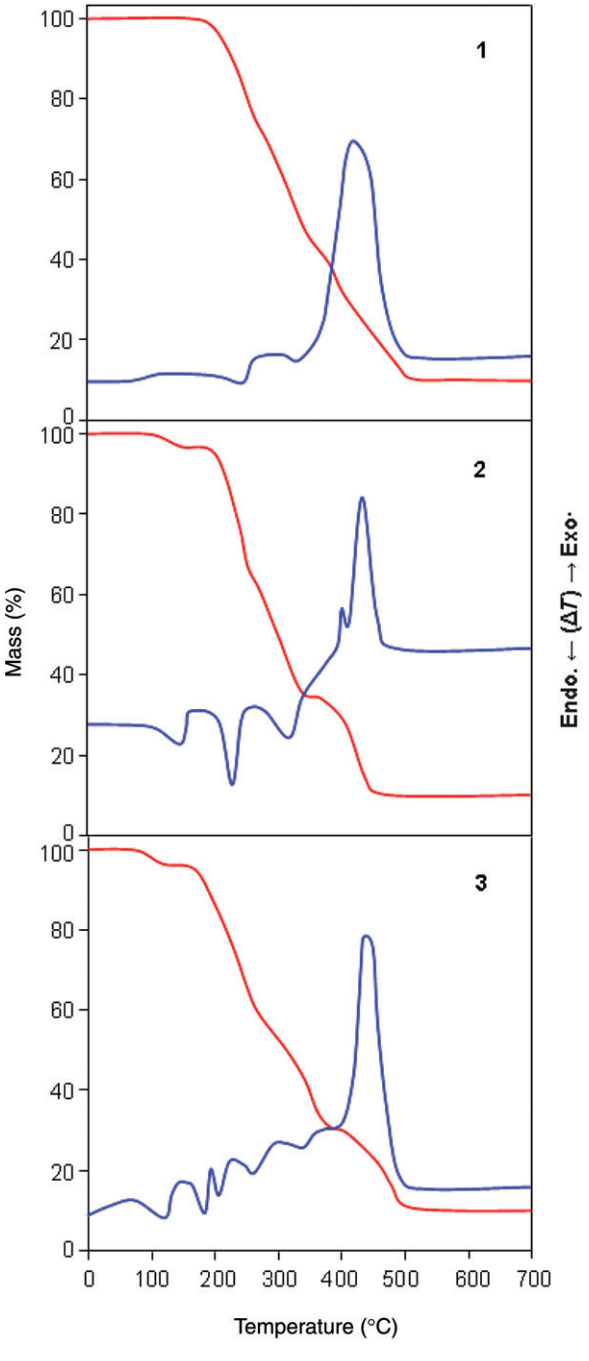

Figure 5. DTA and TG curves of **1**–**3**.

4. Conclusion

The syntheses, characterization, and crystal structures of three new complexes of 5,5-diethylbarbiturate with co-ligands (2-aminomethyl)pyridine, (2-aminoethyl)pyridine, and (2-hydroxyethyl)pyridine are reported. In **1**–**3**, all co-ligands are bidentate chelating, while barb is monodentate (N or O), bidentate, and a counterion. New coordination modes of barb were observed in complexes containing (2-aminomethyl)pyridine and (2-hydroxyethyl)pyridine. All complexes are fluorescent arising from py-based π–π^* transitions.

Supplementary material

CCDC 789905, 789906, and 789907 contain the supplementary crystallographic data for **1**, **2**, and **3**, respectively. These data can be obtained free of charge from the Cambridge Crystallographic Data Centre *via* www.ccdc.cam.ac.uk/data_request/cif.

References

[1] A.W. Dox. *J. Am. Chem. Soc.*, **53**, 1559 (1931).
[2] W.J. Doran. In *Medicinal Chemistry IV*, F.F. Blicke, R.H. Cox (Eds), John Wiley, New York (1959).
[3] Y. Martin-Biosca, S. Sagrado, R.M. Villanueva-Camanas, M.J. Medina-Hernandez. *J. Pharm. Biomed. Anal.*, **21**, 331 (1999).
[4] D.A. Williams, T.L. Lemke (Eds.). *Foye's Principles of Medicinal Chemistry*, 5th Edn, L. Williams Wilkins, Philadelphia (2002).
[5] F. Bortolotti, G.D. Paoli, R. Gottardo, M. Trattene, F. Tagliaro. *J. Chromatogr. B*, **800**, 239 (2004).
[6] B.C. Wang, B.M. Craven. *Chem. Commun.*, 290 (1971).
[7] L.R. Nassimbeni, A. Rodgers. *Acta Cryst.*, **B30**, 2593 (1974).
[8] M.R. Caira, G.V. Fazakerley, P.W. Linder, L.R. Nassimbeni. *Acta Cryst.*, **B29**, 2898 (1973).
[9] G.V. Fazakerley, P.W. Linder, L.R. Nassimbeni, A.L. Rodgers. *Inorg. Chim. Acta*, **9**, 193 (1974).
[10] J. Fawcett, W. Henderson, R.D.W. Kemmitt, D.R. Russell, A. Upreti. *J. Chem. Soc., Dalton Trans.*, 1897 (1996).
[11] N. Haque, J.N. Roedel, I.-P. Lorenz. *Z. Anorg. Allg. Chem.*, **635**, 496 (2009).
[12] F. Yilmaz, V.T. Yilmaz, C. Kazak. *Z. Anorg. Allg. Chem.*, **631**, 1536 (2005).
[13] M.S. Aksoy, V.T. Yilmaz, O. Buyukgungor. *J. Coord. Chem.*, **62**, 3250 (2009).
[14] V.T. Yilmaz, F. Yilmaz, H. Karakaya, O. Buyukgungor, W.T.A. Harrison. *Polyhedron*, **25**, 2829 (2006).
[15] V.T. Yilmaz, E. Soyer, O. Buyukgungor. *Polyhedron*, **29**, 920 (2010).
[16] F. Yilmaz, V.T. Yilmaz, E. Soyer, O. Buyukgungor. *Inorg. Chim. Acta*, **363**, 3165 (2010).
[17] V.T. Yilmaz, M.S. Aksoy, O. Sahin. *Inorg. Chim. Acta*, **362**, 3703 (2009).
[18] L. Nassimbeni, A. Rodgers. *Acta Cryst.*, **B30**, 1953 (1974).
[19] G.M. Sheldrick. *Acta Cryst.*, **A64**, 112 (2008).
[20] T. Chattopadhyay, A. Banerjee, K.S. Banu, E. Suresh, M. Netahji, G. Birarda, E. Zangrando, D. Das. *Polyhedron*, **27**, 2452 (2008).